The Large UV/Optical/Infrared Surveyor (LUVOIR): Decadal Mission Concept Design Update

Matthew R. Bolcar*[a], Steve Aloezos[a], Vincent T. Bly[a], Christine Collins[a], Julie Crooke[a], Courtney D. Dressing[b], Lou Fantano[a], Lee D. Feinberg[a], Kevin France[c], Gene Gochar[a], Qian Gong[a], Jason E. Hylan[a], Andrew Jones[a], Irving Linares[a], Marc Postman[d], Laurent Pueyo[d], Aki Roberge[a], Lia Sacks[a], Steven Tompkins[a], Garrett West[a]

[a]NASA Goddard Space Flight Center, 8800 Greenbelt Rd., Greenbelt, MD, 20771 USA;
[b]Astronomy Dept., 501 Campbell Hall #3411, University of California, Berkeley, CA 94720, USA;
[c]Laboratory for Atmospheric and Space Physics, University of Colorado, Boulder CO 80309, USA;
[d]Space Telescope Science Institute, 3700 San Martin Drive, Baltimore, MD 21218, USA

ABSTRACT

In preparation for the 2020 Astrophysics Decadal Survey, NASA has commissioned the study of four large mission concepts, including the Large Ultraviolet / Optical / Infrared (LUVOIR) Surveyor. The LUVOIR Science and Technology Definition Team (STDT) has identified a broad range of science objectives including the direct imaging and spectral characterization of habitable exoplanets around sun-like stars, the study of galaxy formation and evolution, the epoch of reionization, star and planet formation, and the remote sensing of Solar System bodies. NASA's Goddard Space Flight Center (GSFC) is providing the design and engineering support to develop executable and feasible mission concepts that are capable of the identified science objectives. We present an update on the first of two architectures being studied: a 15-meter-diameter segmented-aperture telescope with a suite of serviceable instruments operating over a range of wavelengths between 100 nm to 2.5 μm. Four instruments are being developed for this architecture: an optical / near-infrared coronagraph capable of 10^{-10} contrast at inner working angles as small as 2 λ/D; the LUVOIR UV Multi-object Spectrograph (LUMOS), which will provide low- and medium-resolution UV (100 – 400 nm) multi-object imaging spectroscopy in addition to far-UV imaging; the High Definition Imager (HDI), a high-resolution wide-field-of-view NUV-Optical-IR imager; and a UV spectro-polarimeter being contributed by Centre National d'Etudes Spatiales (CNES). A fifth instrument, a multi-resolution optical-NIR spectrograph, is planned as part of a second architecture to be studied in late 2017.

Keywords: space telescopes, ultraviolet, optical, infrared, coronagraphy, ultra-stable systems

1. INTRODUCTION

In 2016, NASA's Science Mission Directorate Astrophysics Division commissioned the study of four large mission concepts in preparation for the 2020 Decadal Study[1]: the Large UV/Optical/Infrared Surveyor (LUVOIR), the Habitable Exoplanet Imager (HabEx), the Origins Space Telescope (OST, formerly the Far-Infrared Surveyor), and Lynx (formerly the X-ray Surveyor). Each study is guided by a Science and Technology Definition Team (STDT) charged with defining a compelling science case for the mission. The LUVOIR Study Office at NASA's Goddard Space Flight Center (GSFC) has worked with the LUVOIR STDT to develop the first of two feasible and executable mission architectures, capable of achieving the science objectives identified by the STDT. In this paper, we report on the progress of this study.

The paper is organized as follows: The remainder of Section 1 briefly outlines the LUVOIR science case, and discusses the design philosophy adopted by the LUVOIR STDT and Study Office. Section 2 provides a top-level summary of the LUVOIR Architecture "A" mission elements. Section 3 describes the Optical Telescope Element (OTE), while Sections 4-7 provide details on the instrument suite. Section 8 discusses the LUVOIR spacecraft system, including the sunshield. Finally, Section 9 describes future plans.

1.1 Science with LUVOIR

LUVOIR's STDT has developed a compelling science case that appeals to a broad section of the astrophysics community with three main themes: cosmic origins, exoplanets, and the Solar System.

*matthew.bolcar@nasa.gov; phone 1 301 286-5237; fax 1 301 286-0204; www.nasa.gov/goddard

The cosmic origins science case is defined by the desire for a breadth of observational capabilities at unprecedented sensitivity and resolution. This desire extends from the experience gained with the Hubble Space Telescope (HST), whereby some of the most iconic discoveries made where never initially imagined as science objectives for HST. As HST has demonstrated, a capable, flexible, and upgradeable observatory allows us to answer tomorrow's questions that we don't even know to ask today. These questions range in topic and in scale from "How do stars and planets in our local neighborhood form?" to "How do nearby galaxies evolve and interact?" to "What is the lifecycle of baryons across cosmic time?" Fundamentally, these cosmic origins questions are of the nature, "How did we come to be?"

Complementary to the cosmic origins science, the exoplanet science seeks to answer the question, "Are we alone?" Answering this question requires the ability to directly image habitable exoplanets around sun-like stars, and characterize their atmospheres with spectroscopy. However, LUVOIR doesn't just seek to determine *if* life is present elsewhere, but also *how common* life might be throughout the galaxy. Thus, the need for a sensitive and agile system capable of observing hundreds of planetary systems to determine what fraction of them are habitable (or perhaps, inhabited). During this search, hundreds of other planets would be observed and characterized, allowing for a complete census of the "exoplanet zoo".

Finally, the same capabilities that enable the cosmic origins and exoplanet science would also enable groundbreaking observations closer to home, with the ability to image the planets within our solar system with resolutions previously achievable only by planetary probe missions. LUVOIR would turn these formerly once-in-a-lifetime science campaigns into the routine, while simultaneously enabling new observations of comets, asteroids, and Kuiper belt objects.

These compelling science objectives clearly define a set of high-level mission capabilities: sensitivity, resolution, flexibility, high-contrast imaging, and mission duration. The LUVOIR Study team has used these capabilities to define a set of fundamental requirements that include: a large (8-16 meter) aperture; broad wavelength sensitivity (~100 nm – ~2.5 μm); a suite of upgradeable instruments with imaging, spectroscopic, and high-contrast capabilities; and a long mission lifetime enabled through on-orbit servicing.

1.2 LUVOIR Study Philosophy

The goal of the LUVOIR design study is to develop a mission concept that achieves the science objectives described in Section 1.1, subject to traditional engineering and programmatic constraints of mass, volume, cost, schedule, technical risk, etc. Ultimately, the 2020 Decadal Survey Committee will evaluate LUVOIR and the other mission concepts on these merits: is the science compelling?; is the mission executable and feasible?; and does its science yield justify the cost and risk? A challenge is introduced when one realizes that at the time the Decadal Committee is performing their evaluation, many of the constraints listed above will be unknown. For example, mass and volume are limited by the capability of the launch vehicle. However, the fleet of available launch vehicles is currently in flux. Existing heavy-lift vehicles like the Delta IV Heavy are being phased out in favor of new vehicles like Space X's Falcon Heavy and NASA's own Space Launch System (SLS). While it is certain that these vehicle will be in operation within the next decade or so, what is less certain are the limits of their capability, the cadence of their launch schedule, and the cost of their service.

Another unknown is the future budgetary environment for NASA. All four missions under study are likely to be multi-billion-dollar large-scale missions, similar in scope to HST, the James Webb Space Telescope (JWST), and the Wide-field Infrared Survey Telescope (WFIRST). While the science cases may fully justify these investments, the available budget may require extremely long and protracted development schedules, potentially reducing the value and increasing the risk to the missions.

Finally, the Decadal Committee will be performing their evaluation just as JWST is coming online and WFIRST is being integrated. It is impossible to predict what discoveries these two missions will make that may change the scientific landscape in the next two decades.

In response to these uncertainties, the LUVOIR STDT has decided to put forth for evaluation two mission architectures that bracket a range of options of varying capability, cost, and risk. Architecture "A" is the larger of the two concepts with a 15-m diameter primary mirror that maximizes science yield while accepting moderate technical and programmatic risk. Architecture "A" is the largest, most capable observatory that can be deployed from an anticipated 8.4-m diameter fairing, launched with NASA's SLS Block 2 heavy lift vehicle. Conversely, Architecture "B" represents a more conservative approach where science yield is balanced with technical and programmatic risks. Architecture "B" will be designed to fit within an industry standard 5-m-class fairing, and launched by a vehicle with lift capabilities similar to today's state-of-the-art (~10,000 kg to sun-Earth Lagrange point 2, i.e. SEL2).

These two concepts demonstrate a scaleable mission architecture that can be adapted to an uncertain future. When taken into consideration along with the HabEx Study's[2] 4-m monolith and 6.5-m segmented architectures, there are a continuum of options between 4-m and 15-m apertures with a range of science yield, cost, and technical risks.

2. LUVOIR ARCHITECTURE "A" OVERVIEW

2.1 Design Overview

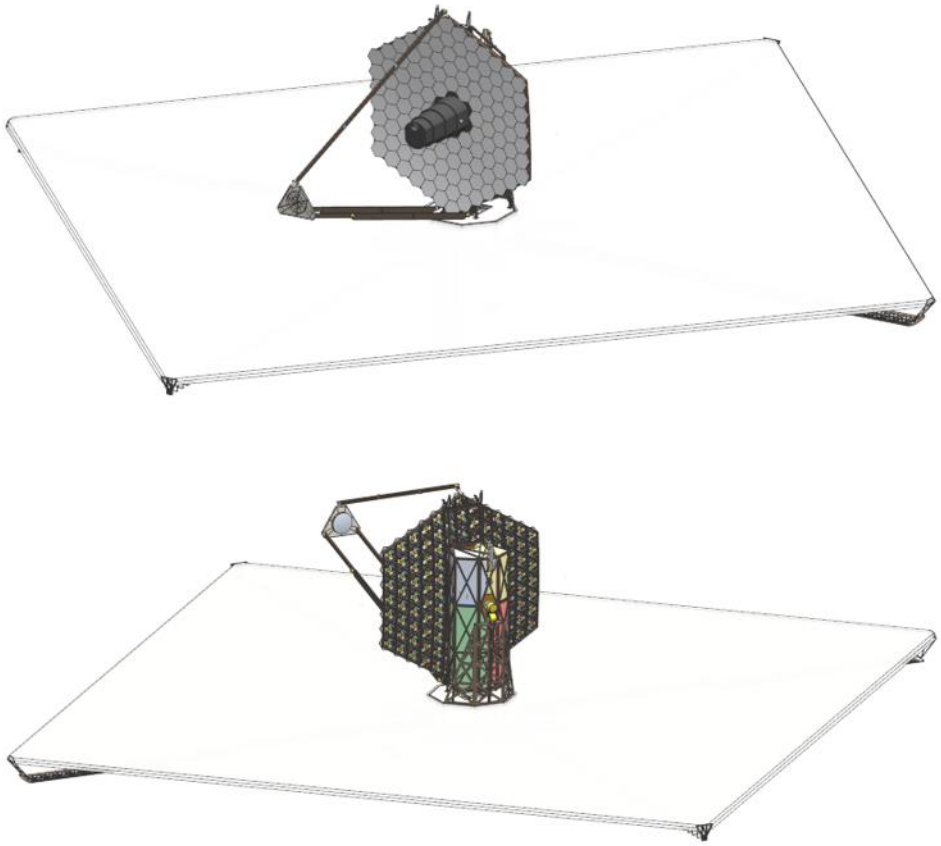

Figure 1 – Front and back views of the LUVOIR observatory. The front view shows the primary mirror, secondary mirror support structure, and the deployable aft-optics support structure (black telescoping structure near the center of the primary mirror). The rear view shows the backplane support frame (BSF), holding the four instruments, depicted here as simple colored volumes: LUMOS (green), HDI (red), Coronagraph (blue), and Pollux (yellow). The two-axis gimbal is also visible near the middle of the BSF. The spacecraft bus is hidden below the sunshield, which is ~53-m on an edge. This figure shows the observatory at gimbal angle "90°". At gimbal angle "0°", the telescope is pointing up, with the boresight perpendicular to the sunshield.

The LUVOIR Architecture "A", shown in Figure 1, draws on heritage from HST, JWST, and WFIRST. Similar to HST, LUVOIR covers a bandpass spanning the far-UV (FUV) to the near infrared (NIR), has a suite of imagers and spectrographs, and perhaps most importantly, is designed to be serviceable and upgradeable. Like JWST, LUVOIR has a segmented primary mirror that deploys from a stowed configuration, along with the secondary mirror support structure (SMSS) the sunshield, and a number of other subsystems. Finally, like WFIRST, LUVOIR has a high-contrast coronagraph instrument, capable of directly imaging and spectroscopically characterizing habitable exoplanets. In this sense, LUVOIR builds upon the technical legacy of the great space observatories that have preceded it.

The LUVOIR Architecture is divided into three primary systems: the Flight System consisting of the observatory itself, the Ground System consisting of ground stations and mission and science operations centers (MOCs, SOCs), and the Launch Vehicle. The Flight System is further divided into the Payload and the Spacecraft. Figure 2 shows the Flight System and identifies key subsystems. In the following sections, we highlight several important aspects of the overall mission architecture.

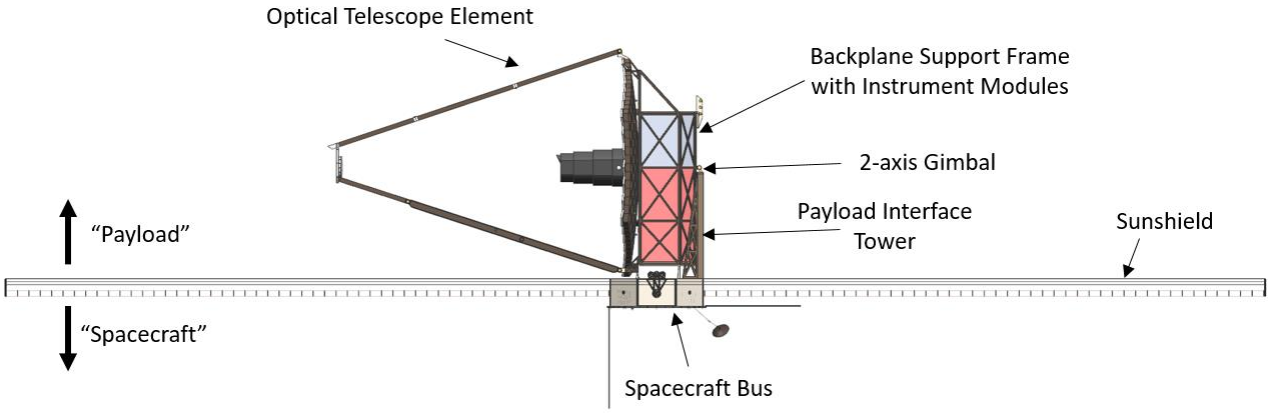

Figure 2 – The LUVOIR Flight System, with identified subsystems. Everything above the sunshield (with the exception of the payload interface tower) is considered part of the payload. The payload interface tower, the sunshield, and everything below the sunshield are collectively considered the spacecraft.

Wavefront Stability for High-contrast Imaging:

While LUVOIR is intended to be a multi-purpose, multi-user observatory, the desire to perform high contrast (10^{-10}) direct imaging of habitable exoplanets drives almost every aspect of the architecture. It has been shown[3,4,5] that achieving such contrast levels with an internal coronagraph requires wavefront stability of the end-to-end optical system on the order of 10s of picometers over the spatial frequencies corresponding to the dark-hole region in the focal plane, and over time periods corresponding to the wavefront control bandwidth. The approach to achieving picometer-level stability on LUVOIR is three-fold:

High-contrast Through Ultra-stable Systems: With this approach, we've designed a system that is as stable as possible. Thermal stability is achieved using materials with near-zero coefficient of thermal expansion (CTE) at the nominal operating temperature of 270 K: Corning ULE® mirror segment substrates[6] and zero-CTE composite material structures[7]. These materials are coupled with milli-Kelvin-level thermal sensing and control of the mirrors, structures, and critical interfaces. Dynamic stability is achieved with passive isolation at the disturbance sources, and a non-contact Vibration Isolation and Precision Pointing System (VIPPS) that actively isolates the payload from the spacecraft[8]. Material property characterization is critical to understanding the behavior of structures and interfaces and modeling their performance at the picometer level. Ground-based metrology systems that can verify model predictions is also necessary.

High-contrast Through Wavefront Control: This approach reduces the time period over which the system must be stable by increasing the temporal bandwidth of the wavefront control system. Slow, low-order drifts in the wavefront error are sensed and corrected with a low-order wavefront sensor (LOWFS) similar to the one to be used on WFIRST[9]. The LOWFS system, however, is fundamentally limited in which wavefront terms are sensed, and how fast they can be sensed. Higher-order wavefront error terms will be sensed with an out-of-band wavefront sensor. At the same time, fast dynamic motions of the primary mirror segments will be measured using edge sensors and corrected with piezo-electric (PZT) actuators[10].

High-contrast Through Wavefront Tolerance: This approach attempts to relax the fundamental stability requirement from 10s of picometers to 100s of picometers, or even nanometers, through new coronagraph architectures that are designed to be less sensitive to the wavefront error modes that are most prominently excited in the LUVOIR

architecture[11,12]. Additionally, spatial filtering techniques are being explored that may enable additional orders-of-magnitude in contrast, further relaxing the stability requirement[13].

Thermal Design:

The thermal architecture of the observatory plays a critical role in achieving the necessary wavefront stability. The choice of materials and the material properties work together to create a system that is both thermally stable and controllable at the observatory operating temperature. The nominal 270 K operating temperature represents a balance between operating at a cold enough temperature to achieve low thermal backgrounds in the NIR science bands, while operating warm enough to help mitigate contamination concerns in the UV science bands. Evidence from JWST thermal testing shows that below 260 K, molecular species rapidly begin to deposit on surfaces, which would degrade UV throughput[14]. Thus, 270 K was a compromise to maximize NIR science while not significantly impacting UV science.

Separately from science considerations, 270 K was also chosen for a number of engineering reasons[14]. At warmer temperatures, damping of dynamic disturbances is increased. Also, the selection of materials that have both near-zero CTE and that are also well characterized is larger near room temperature. Finally, a warmer temperature was chosen to help reduce the complexity of fabrication, integration, and test campaigns. By fabricating components at a temperature near where they are to be operated, modeling error can be reduced, as well as the complexity, number, and duration of thermal cycle tests.

In order to maintain a stable 270 K temperature, the observatory must first be cold-biased, necessitating a large sunshield similar to JWST's. Heaters are then used to raise the temperature from the cold-bias and precisely control the temperature throughout the observatory. Heater power is the largest drawback to maintaining a warm telescope and structure. Even so, the ~10 kW current best estimate (CBE) power requirement for the entire observatory is well within the capability for a reasonably sized solar array.

Sunshield:

A large, planar sunshield is used to shadow the optical payload from stray light from the sun, Earth, and moon, while also thermally isolating the optical payload to provide a cold bias. The sunshield is designed to provide a temperature of ~60 K on the anti-sun side. This temperature also provides a cold sink for several radiators mounted to the instrument structure that are used to passively cool NIR detectors to 70 K, and which have a direct view of the sunshield for specific payload pointing vectors.

Nominally, the sunshield remains at a fixed angle perpendicular to the sun-earth axis during science observations, yielding a very stable thermal environment on the anti-sun side. However, for special solar system or time-critical exoplanet revisit observations, the entire observatory can be tipped toward the sun for viewing angles up to ~40° solar elongation. The sunshield is sized such that the entire optical payload will remain in shadow during such maneuvers, although the thermal environment will clearly be changed. Analysis is currently underway to estimate thermal settling times during such maneuvers.

Gimbal and Vibration Isolation & Precision Pointing System (VIPPS):

The optical payload is articulated with respect to the spacecraft using a two-axis gimbal system. Repointing the observatory involves rolling the entire observatory about the sun-earth axis through 360°, while simultaneously pitching the payload with the gimbal from 0° to 90°. With these two degrees of freedom, the payload can point anywhere in the anti-sun hemisphere. An additional second axis on the gimbal allows just the payload to roll about the telescope boresite from 0° to 90°. The boresite roll allows targets to be aligned to instrument-specific apertures, as well as enabling point-spread function (PSF) roll subtraction.

The Vibration Isolation and Precision Pointing System (VIPPS) is a non-contact dynamic isolation system that separates the payload from the spacecraft. The system "floats" the telescope and controls the payload attitude relative to the interface plane via six non-contact voicecoil actuators. The VIPPS effectively isolates any dynamic disturbances from the spacecraft attitude control system (ACS) from transmitting to the payload and exciting resonances that contribute to wavefront instability. The VIPPS also provides fine pointing control of the payload during science observations. For a more detailed discussion of the VIPPS and its performance, the reader is referred to Dewell, *et al*[8].

While the VIPPS provides ideal mechanical isolation, power and data signals must still be transmitted between the payload and spacecraft. By using a 120-v bus for the electrical power system (EPS), fewer, smaller-gauge conductors can be used,

minimizing the number of cables and cable stiffness that must bridge the non-contact isolation system. Similarly, by performing as much of the data-processing on the payload side as possible, the cabling requirements for data transfer between the payload and spacecraft are minimized to fewer than 10 SpaceWire cables, which includes redundancy and cross-strapping. Analysis is currently underway to determine the impact the power and data cables have on the VIPPS performance.

Serviceability:

Drawing on the legacy of HST, LUVOIR is being designed from the outset to be serviceable and upgradeable to enable a multi-decade science mission that is responsive to a changing scientific landscape. Thus, the reliability, lifetime, and consumables have been designed to meet a 5-year minimum lifetime for all mission elements, a 10-year goal lifetime for all serviceable or replaceable mission elements, and a 25-year goal lifetime for all non-serviceable/replaceable elements.

The serviceable elements on the observatory include the four instrument modules themselves. Throughout the study, the instruments were designed to be as self-contained as possible. All electronics, software, and thermal control hardware are contained within a single instrument module. Thus, the only interface between the instrument and the payload (aside from mechanical) is a 28 V power bus, a SpaceWire connection for science data downlink, and a 1553 bus for telemetry. Each instrument has its own command and data handling (C&DH) unit for collecting, processing, and preparing data for downlink. Each instrument also has enough internal storage for two days' worth of continuous data collection. With downlinks planned twice daily, the internal storage provides adequate margin against potential missed downlink passes.

The spacecraft is also designed with 8 orbital replacement units (ORUs). Four of these ORUs contain the attitude control system (ACS) control moment gyroscopes (CMGs). The other four contain other spacecraft subsystems such as communications, electrical power (including a battery), and avionics, all of which can be completely replaced and upgraded by changing out the ORU. Each ORU also holds one of eight solar panels, allowing the solar array to also be upgraded and replaced during the mission lifetime.

The main elements of the observatory that have not been designed to be serviced include the optical telescope element (OTE) itself, the backplane support frame (BSF) which acts as the metering structure between the OTE and the instruments, and the sunshield.

Launch Vehicle:

As discussed in Section 1.2, the LUVOIR Architecture "A" has been designed to take full advantage of NASA's SLS Block 2 vehicle. Several payload fairings (PLFs) have been proposed for this launch vehicle[15]: an 8.4-m diameter "short" (19.1-m tall) fairing, an 8.4-m "long" (27.4-m tall) fairing, and a 10-m x 27.4-m fairing. As the capabilities of the SLS Block 2 and its user base are still evolving, so is the certainty of which of the fairings will actually be developed. The

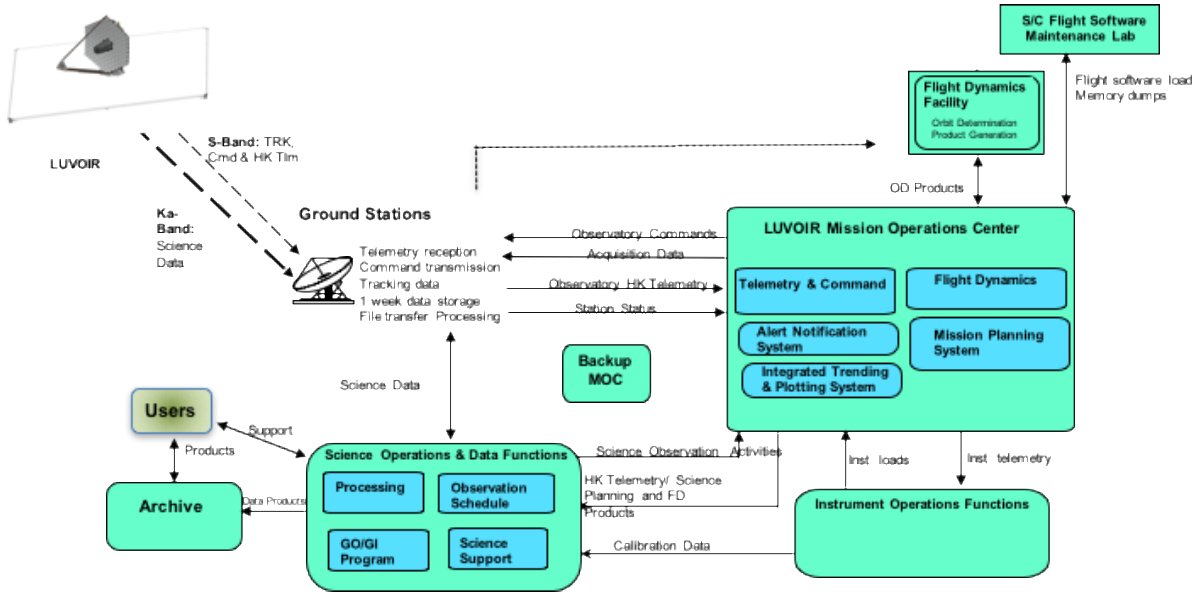

Figure 3 – A notional LUVOIR Ground System.

LUVOIR team opted to be conservative in the fairing diameter and chose the 8.4-m "long" PLF (the "short" version does not provide enough height under the ogive to fit a > 7-m aperture).

Based on the latest revision of the SLS Mission Planner's Guide[15], the lift capacity for the SLS Block 2 configuration with the 8.4-m "long" PLF is 44.3 metric tons.

Ground System:

The LUVOIR Ground System will be based on the successful models of other large observatories such as HST and JWST. Primary and backup mission operations centers (MOCs) will be responsible for overall control of the observatory, orbit determination, telemetry, and mission planning. Similarly, a science operations center (SOC) will be responsible for planning the observation schedule, supporting a guest-observer (GO) program, processing science data, and distributing and archiving the data for the user base. Two Ka-band ground stations are also baselined to provide two downlink passes per day. The ground stations consist of 18-m dishes in White Sands, NM, and in South Africa. Figure 3 shows a schematic of the LUVOIR Ground System.

3. OPTICAL TELESCOPE ELEMENT

3.1 Science Overview and Capabilities

As the primary interface between the instrument suite and the astronomical objects being observed, the optical telescope element (OTE) must be capable not just of achieving all of the science objectives identified by the STDT, but also science objectives that have not yet been imagined. And since the OTE is one of the mission elements that is not intended to be serviceable, it must be reliable and robust. The breadth of the science case discussed in Section 1.1 implies a set of high-level capabilities for the OTE: sensitivity, resolution, stability, flexibility, and agility. Combining these capabilities with constraints such as mass, volume, and technical readiness, the Study Team has mapped these capabilities onto a set of performance specifications, shown in Table 1.

Table 1 – Performance specifications for the LUVOIR "A" OTE, derived from science capabilities.

Specification	**Value**	**Mapped Capabilities**
Aperture Diameter	15 meters	Sensitivity, Resolution, Flexibility
Field-of-View	15 arcmin × 8 arcmin	Flexibility, Agility
Wavelength Range*	100 nm – 2.5 μm	Sensitivity, Flexibility
Reflectivity	> 60% at 105 nm > 90% at 115 nm Average ~ 90% between 400 and 850 nm Average > 95% between 850 nm and 2.5 μm	Sensitivity, Flexibility, Agility
Static Wavefront Error†	< 35 nm RMS	Resolution, Stability
Pointing Stability‡	± 0.97 mas 1-σ per axis over an observation	Resolution, Stability
Object Tracking+	60 mas / s	Flexibility, Agility
Slew Rate+	Required: Repoint anywhere in anti-sun hemisphere in 45 minutes Goal: Repoint anywhere in anti-sun hemisphere in 30 minutes	Agility

**The blue end of the wavelength range is limited by the coating performance, while the red end is limited by the telescope thermal background; longer wavelengths can be observed for sufficiently bright objects. †The static wavefront error is the end-to-end optical performance, including that of the instrument. To achieve an end-to-end 35 nm RMS wavefront error, the contribution from the OTE itself would necessarily need to be lower. ‡The pointing stability here is the requirement at the OTE focal plane, and is achieved by a tiered approach incorporating the fine steering mirror, VIPPS, and spacecraft attitude control system. +Object tracking and slew rates levy requirements on the VIPPS and attitude control system, however we include them here for a complete picture of the OTE's capabilities.*

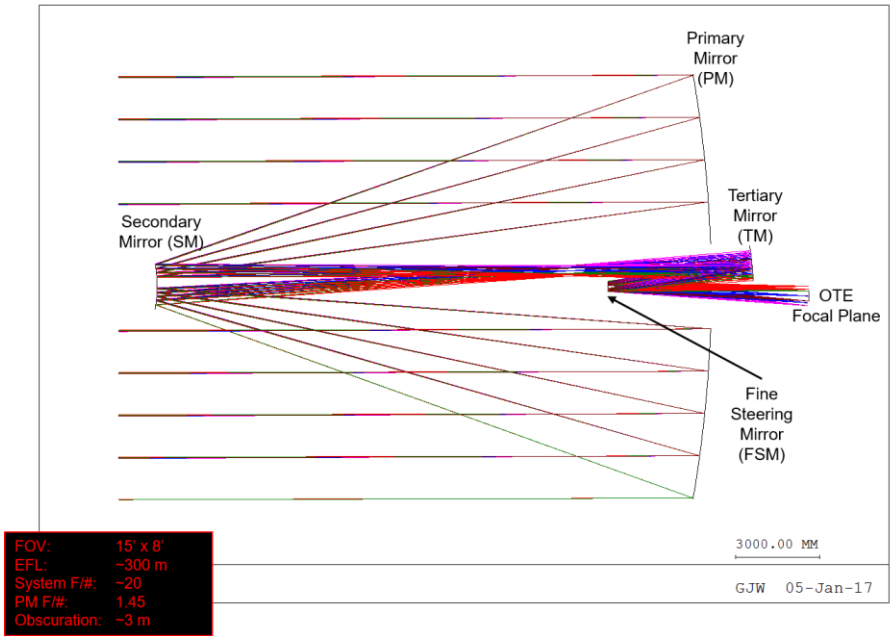

Figure 4 – LUVOIR OTE optical design. First-order optical parameters are shown in the inset.

As discussed in Section 2.1, the wavefront error stability needed to achieve the high-contrast exoplanet science is a critical requirement that drives the OTE design. The material choices, thermal control system, segment-level architecture, segment phasing concept, and secondary mirror support structure are all impacted by the need to maintain wavefront stability at the picometer level. A discussion follows in the next section, but the reader is referred to Feinberg, *et al.* for a more detailed discussion of achieving ultra-stability with the LUVOIR observatory[10].

3.2 Design Overview

Optical Design and Performance

The LUVOIR OTE was designed as a three-mirror anastigmat (TMA) system, with a fourth fine steering mirror (FSM) located at the real exit pupil of the OTE. The advantages of this system include a wide field-of-view that can be accessed by a number of instruments, with spherical, coma, and astigmatism aberrations corrected. The inclusion of the FSM also allows for ultra-fine pointing stability to be achieved by all of the instruments, and relaxes some of the requirements on the VIPPS to point the massive science payload. The biggest disadvantage of this system is the two additional reflections that are needed (tertiary mirror, FSM) before light enters any ultraviolet channels. However, this throughput reduction is more than compensated by both the collecting area of the telescope and the high reflectivity of the coating at UV wavelengths. Figure 4 shows a ray trace of the OTE system, and Figure 5 shows a wavefront error map over the telescope's field-of-view, with each instrument's field-of-view superimposed.

As the optical design evolved, it became clear that a sizeable central hole in the primary mirror was needed to pass the ray bundle through the aft-optics system (AOS). The minimum achievable clearance hole was 2.7 m; the secondary mirror obscuration is entirely contained within this diameter. To optimally pack the mirror segments around this hole and minimize unused collecting area, while also maintaining the outer diameter of the primary mirror in the 15-16 meter range, a segment size of 1.15 m flat-to-flat was selected and arranged in five concentric rings, for a total of 120 segments. Figure 6 shows the LUVOIR aperture, with annotated diameters.

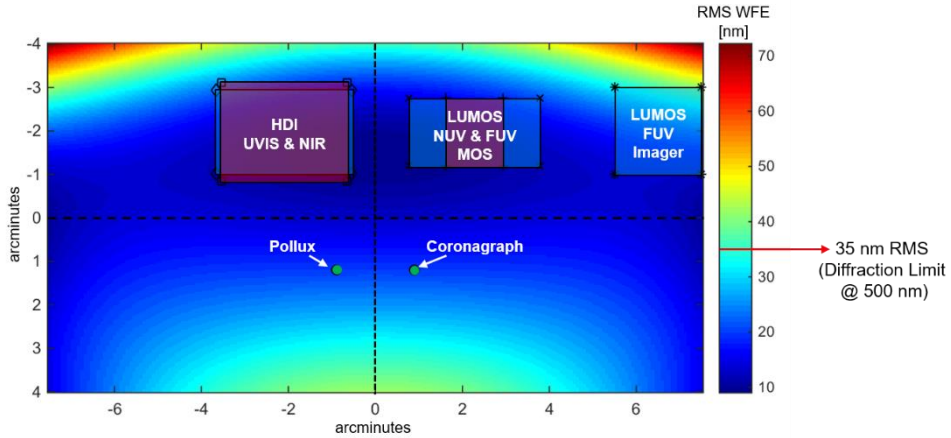

Figure 5 – The RMS wavefront error over the 15 x 8 arcmin OTE FOV. Inset are each of the instrument's fields-of-view.

Mechanical Design & Deployment

The design initially focused on maximizing the primary mirror area while minimizing deployment complexity and being constrained by the SLS PLF volume. The JWST wing-fold deployment was adapted to a dual-wing-fold on each side of the primary mirror, allowing JWST-like deployment mechanisms, hinges, and latches to be used on LUVOIR. The dual-wing-fold geometry also allows the primary mirror to more conformally match the circular diameter of the fairing, allowing more volume in the center of the fairing for the instrument stack. Similarly, the JWST single-hinge secondary mirror support structure (SMSS) deployment was adapted for LUVOIR, with two additional hinge points on the top beam of the SMSS. Finally, the aft-optics support structure (AOSS) was made to be deployable using a nesting-telescoping structure, similar to a collapsible camp cup.

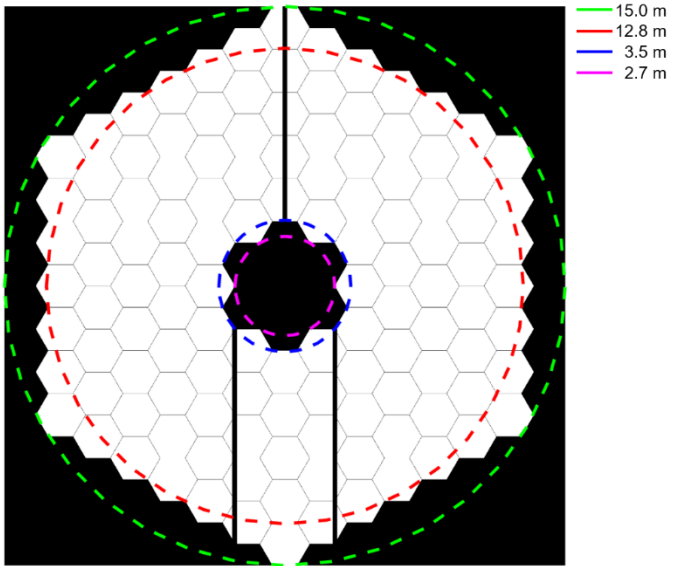

Figure 6 – The LUVOIR entrance pupil aperture. There are 120 segments, each 1.15 m flat-to-flat, with 6 mm gaps. Inscribed and circumscribed diameters are shown for reference.

Primary Mirror Segment Assembly (PMSA)

The PMSA architecture also heavily leverages JWST heritage. A single, stiff mirror segment is mounted on a hexapod for 6 degree-of-freedom (DOF) rigid-body positioning of the segment. A whiffle structure and delta frame interfaces the mirror segment substrate to the hexapod actuators and to the primary mirror backplane structure (PMBS). Where the LUVOIR PMSA architecture departs from that of JWST is primarily in the materials. Instead of beryllium segments, LUVOIR has baselined Corning's Ultra-low Expansion (ULE®) glass for the mirror substrate. Additionally, LUVOIR's delta frame and whiffle will be zero-CTE composite material. LUVOIR is also not baselining the use of a radius-of-curvature (RoC) adjustment actuator. It is believed that adequate RoC matching can be achieved during segment polishing, and the additional mass and complexity of the actuator is not required.

Another area of departure from the JWST PMSA architecture is the incorporation of an active thermal control system for each of LUVOIR's mirror segments. A heater plate immediately behind the glass substrate radiatively heats the mirror segment to 270 K ± 1 mK[6]. The PMBS is also actively heated at key control points in order to maintain the global thermal stability of the primary mirror. For more details on the LUVOIR thermal control concepts, the reader is referred to Park, *et al*[7].

Finally, a critical new component to the PMSA architecture is the edge sensor-PZT actuator control system. Each mirror segment is fitted with one edge sensor per edge (i.e. two edge sensors total per shared edge for a total of 622 across the LUVOIR aperture). While the current design baselines capacitive-based edge sensors, optical or inductive sensors could also be used if sufficiently mature and capable. Each edge sensor measures local gap, shear, and dihedral angle. Incorporating these three measurements from all 622 sensors allows for a global solution to be found for the six DOF position of each segment, relative to a reference. The 6 DOF positions are fed back to the hexapod fine-stage PZT actuators to control the segment position with picometer resolution[10].

4. UV-OPTICAL-NIR CORONAGRAPH

4.1 Science Overview and Capabilities

The scientific goals of the coronagraph instrument are commensurate with the ambitious philosophy underlying the LUVOIR Architecture "A" and is organized around two key science themes: (1) measuring the occurrence rate of biomarkers in the atmospheres of rocky planets orbiting in the Habitable Zone (HZ) of their host stars, and (2) studying the diversity of exo-planetary systems. The former science theme is significantly more stressing on the instrument and drives the trades we studied to design the LUVOIR coronagraph instrument. Any mission aimed at measuring the occurrence rate of biomarkers in the atmosphere of nearby HZ rocky planets, ought to first be capable of detecting a statistically significant ensemble of exo-earth candidates[16]. The detectability of exoplanets in long coronagraph exposures

depends on both the level of contrast achieved in the high-contrast region (Dark Hole, DH) of the focal plane, and on the on-axis throughput of the coronagraph at the apparent separation of the planets, expressed using the Inner and Outer Working Angle (IWA and OWA) scalar metrics.

The characterization of identified exo-earth candidates is equally as important as their detection. Figure 7 shows a simulated spectrum of a mature earth along with a 2-Gyrs-old Archean earth generated with the LUVOIR STDT online exoplanet spectrum simulation tool[17]. This example illustrates the most salient characteristics of the atmosphere of earth analogs which we seek to characterize with great precision using the LUVOIR Architecture "A" coronagraph and translate into the following three requirements on the back-end spectrograph: (1) Continuous spectral coverage from 200 nm to 2.5 μm in order to capture the spectral features associated with carbon and oxygen based molecules, which help discriminate the various atmospheric composition, and (2) spectral resolution of at least R = 150 (and above R = 1000 if possible) in the visible and near-IR. Spectroscopy of faint exo-earths beyond 1.6 μm will be limited to the closest and brightest targets due to the thermal background from the 270 K telescope. Nevertheless, redder spectral coverage will be invaluable to studying the details of the atmospheres of our nearest neighbors, as well as characterizing larger planets. For a more detailed discussion of the coronagraph science case and instrument design, the reader is referred to L. Pueyo, *et al.*[18]

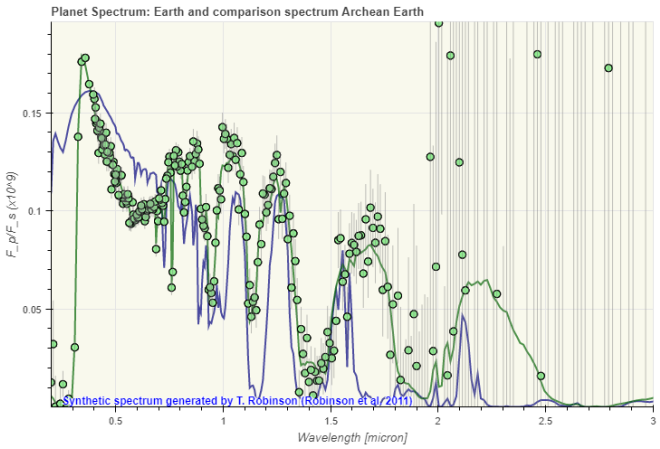

Figure 7 – *Green Line:* A simulated exo-Earth spectrum, *Green Dots*, a simulated R=150 spectrum of the exo-Earth, as collected by the LUVOIR Architecture "A" coronagraph instrument, *Blue Line*: a simulated Archean earth spectrum for comparison. LUVOIR can clearly collect detailed enough spectra to discriminate between these two candidate planets. At wavelengths greater than ~1.8 μm, the telescope thermal background dominates the collected spectra.

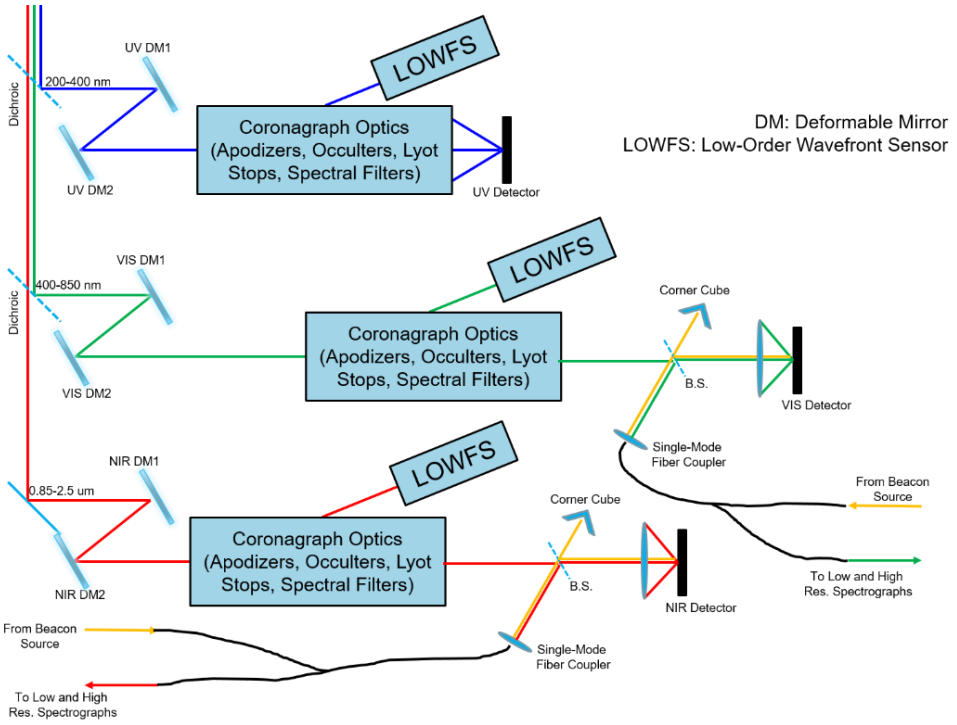

Figure 8 – Block diagram of the coronagraph instrument. Light from the OTE enters in the upper left corner and a sequence of dichroic beamsplitters separates the UV, Vis, and NIR channels of the instrument. Each channel has two DMs for independent wavefront control. Following the DMs, each channel has a series of pupil and image relay optics to allow for the insertion of a variety of apodizing masks, occulting masks, Lyot stops, and spectral filters. Each channel also has a Zernike wavefront sensing LOWFS system that uses light rejected from the occulting mask to sense pointing and low-order wavefront errors. The LOWFS can also operate as an out-of-band wavefront sensor simply by inserting a mirror instead of an occulting mask to direct all of the stellar photons to the wavefront sensor. Finally, each channel has an imaging detector, and the Vis and NIR channels use a fiber injection unit to send planet light to a high-resolution fiber-fed spectrometer (HR-FFS).

4.2 Design Overview

The coronagraph is a complex instrument, as captured in Figure 8. At the top level this complexity stems from the need of having continuous spectral coverage from 200 nm to 2.5 μm. In order to

accommodate the variety of high reflectivity coatings and detector technologies that span such a large wavelength range, the instrument is split into three channels that cover the following bandpasses: UV (200 to 400 nm), optical (400 nm to 850 nm), and NIR (850 nm to 2.5 microns). This is achieved using a series of dichroics at the entrance of the instrument. Each channel is equipped with two deformable mirrors (DMs) for wavefront control, a suite of coronagraph masks, a low-order / out-of-band wavefront sensor (LOWFS[19], OBWFS), and separate science imagers and spectrographs. Each channel also contains a spectral filter wheel mechanism to select the instantaneous bandpass of a particular observation; while the three channels can operate in parallel, each channel can only observe in one bandpass at a time. Figure 9 show a side view of the three spectral channels in their layered configuration, and Figure 10 shows a rendering of the NIR channel of the coronagraph instrument; the visible and UV channels have a similar layout.

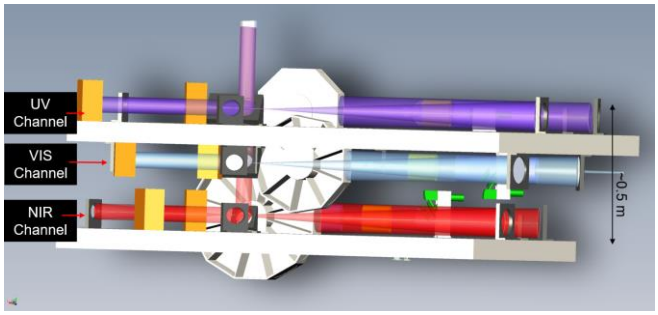

Figure 9 – Rendering of the three spectral channels, arranged in a layered configuration. The instrument is very compact, and squeezes many components and mechanisms into a ~0.5-m tall volume.

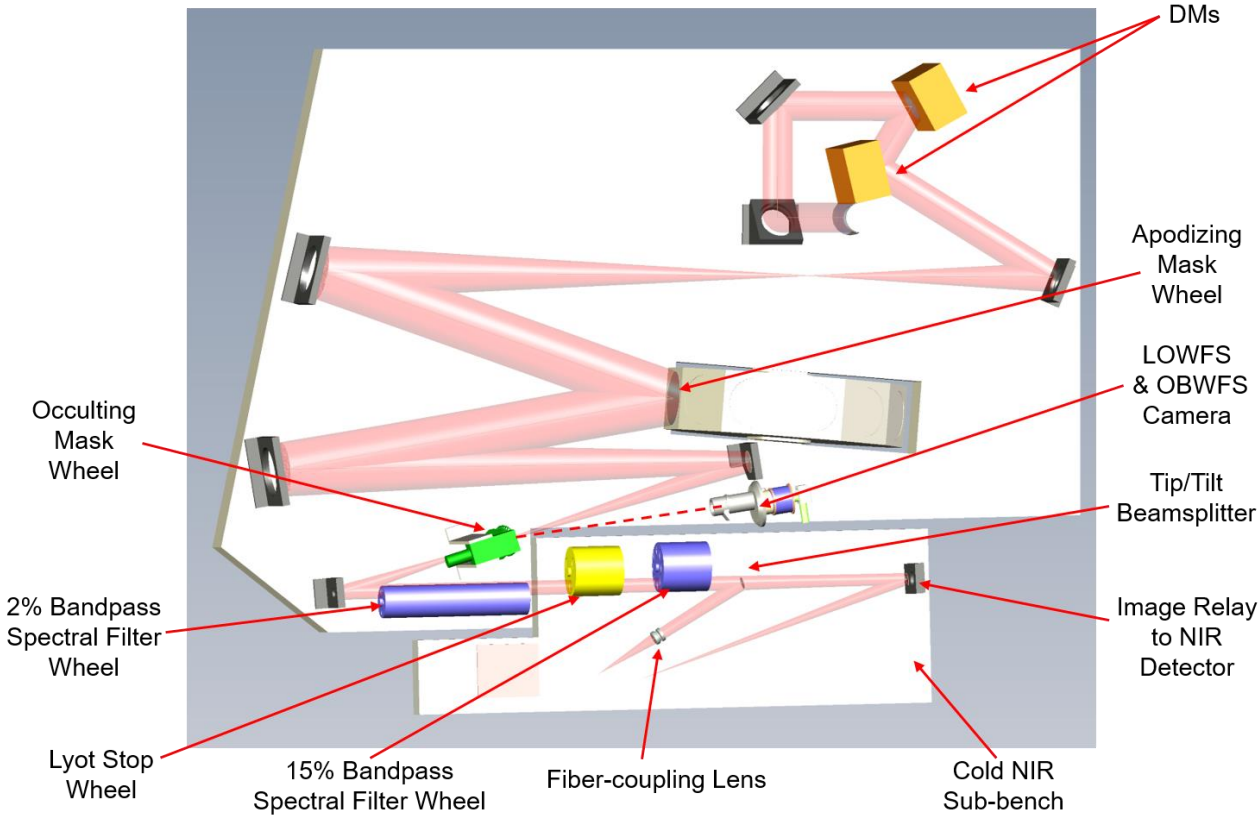

Figure 10 – Top-down view of just the NIR channel of the coronagraph. Light enters from the OTE perpendicular to the plane in the upper right hand corner before being sent to the pair of deformable mirrors. The NIR channel has a thermally isolated sub-bench that runs at a colder temperature to help reduce thermal backgrounds. The UV and Vis channels have very similar layouts.

Detectors

The detector technologies are specific to each channel and our baseline choices heavily rely on technology that has been used on previous missions and/or is planned in the WFIRST baseline instruments:

Visible Channel: The baseline technology for the visible (400 – 850 nm) channel is an e2v EMCCD, with a format of 1024 × 1024, 13 μm pixels. This technology is based on a silicon CCD with a low-noise, on-chip, multiplication gain register (1000× gain). It is the baseline detector for the WFIRST coronagraph instruments. We assumed zero read noise (in photon-counting mode) and a median dark current of 1×10^{-4} e^-/pix/sec (as measure by JPL WFIRST project[20,21]) for our radiometry calculations.

NIR Channel: The baseline technology for the NIR (850 nm – 2.5 μm) is a Teledyne HAWAII 4RG with SIDECAR ASIC, with a format of 4096×4096, 10 μm pixels. It is the baseline detector for the WFIRST wide-field instrument and is an evolution of H2RG detector used on the JWST NIRCam instrument. We assumed a median read noise of ~5 e–/pix, and a median dark current: 2×10^{-3} e^-/pix/sec for our radiometry calculations. It is worth noting there is a possibility the read noise value can be further reduced to 1-2 e^-/pix with additional optimization of the readout circuit.

UV Channel: The UV (200 – 400 nm) channel detector is similar to the visible channel e2v EMCCD, except that the detector surface is δ-doped. We assumed the same performance characteristic as the visible channel detector, however this technology is not fully mature yet and requires some investment.

Back-end Imagers & Spectrographs:

Each channel will be equipped with an imaging detector as described above. Spectroscopy is not required at UV wavelengths and the imager (with a 1.4" × 1.4" field-of-view) is the only science detector. Both an imager and spectrograph are required for the visible and NIR channels. The imager fields-of-view are 2.7" × 2.7" and 5.6" × 5.6", respectively. For the visible and NIR spectrographs we first studied the feasibility of an Integral Field Spectrograph (IFS), similar to those installed on ground based instruments[22,23,24] and the one envisioned for WFIRST[25]. A coronagraphic IFS requires Nyquist sampling the instrument point-spread function (PSF), which means having at least two spatial elements per unit of the angular resolution (two pixels per λ/D). With a 15-m aperture, Nyquist sampling at 600 nm in the visible channel with a spectral resolution of R = 150, requires a 10,000 × 10,000 detector array, a factor of 10 beyond the EMCCD technology that will be matured by WFIRST. This prompted us to also consider a high-resolution fiber-fed spectrograph[26] (HR-FFS). While this solution is less mature, it better uses detector real estate and can potentially yield higher resolution spectra for the brighter planets/most nearby systems (for example, R = 1500 would require a 100,000 × 100,000 detector array in an IFS, but can be achieved with a standard array size in the HR-FFS). We list the pros and cons of each technique below:

IFS pros: This technology will be TRL9 post-WFIRST. It is an intrinsically multiplexed design; the spectrum of multiple planets (or background sources) can be obtained at the same time, making the observations more efficient. The continuum of the planets spectra, essential to measure absolute molecular abundances, is preserved.

IFS cons: Technology development is required to mature low noise 10,000 × 10,000 pixel detectors to achieve the minimum required R=150 spectral resolution, without compromising on instrument field-of-view or bandpass. Obtaining resolutions of R=1500, an option that has been deemed preferable by the LUVOIR STDT Exoplanet Science Working Group, would be exceedingly difficult to achieve with an IFS, even with an additional decade of vigorous detector technology development.

HR-FFS pros: Detector format does not limit spectral resolution as dramatically. Both coherent starlight suppression and post-processing gains using cross-correlation with spectral templates[27,28] are possible with this architecture, potentially relaxing the requirements on the wavefront control system. This technique will be tested in multiple ground based observatories over the next decade[29].

HR-FFS cons: Even if ground-based demonstrations are successful, additional development is necessary to bring this technology to high TRL levels in the context of a space mission. The cross-correlation technique cannot measure absolute molecular abundances and achromatic fiber injection needs to be demonstrated in order to confidently measure the continuum of the planet's spectra. Because the spectrum of only one object at a time can be obtained, the observing efficiency of this design is inferior to that of the IFS.

Based on these trades, the choice of a HR-FFS as the primary spectrograph for the exoplanet imaging of LUVOIR Architecture "A" was mostly driven on scientific considerations: it is the only design that can obtain both low- and high-resolution spectra of earth-analogs, along with being able to characterize a wide variety of other type of planets (including outer planets). However in the absence of a design reference mission at this stage, it is hard to quantify the impact to the science yield that the reduced observing efficiency will have. In particular, the loss of efficiency associated with the inability to spectroscopically vet point source candidates without multiple follow up observations (in order to establish physical association) might have a significant impact on the overall yield. Therefore, an IFS solution is still considered as a back-up for Architecture "A" and will be studied in detail for the Architecture "B" coronagraph instrument (which has a smaller, ~9 m, aperture and therefore is less demanding on detector pixel count).

Mechanisms:

Deformable Mirrors: Our choice of DM technology is based on the need for high-density devices necessary to achieve large OWAs. For instance achieving high contrast for the outer region of the HZ around the most nearby stars requires an OWA of ~48λ/D, which translates into 96 actuators across the pupil. Imaging of outer giant planets drives the actuator count higher, to ~128 actuators across the pupil. In order to keep the optical design compact we baselined a MEMS DM device. A secondary technical driver is the fact that such compact DMs can achieve small Fresnel numbers, and thus are more amenable to DM-based correction of amplitude errors. While this technology will not be matured by WFIRST at the component level, there are avenues to do so using smaller satellites[30].

Element Select Mechanisms: Each of the three channels is equipped with a series of element select mechanisms that accommodate the various apodizing, occulting, and Lyot masks, as well as spectral filters. The number of elements in these mechanisms is driven by two considerations. First, each channel can only operate over an instantaneous 15% spectral bandpass at a time, due to limitations on wavefront control techniques, requiring between six and eight spectral filters per channel. Each of those 15% bands must further be reduced to three 2% bands for collecting the wavefront control images. With additional neutral density filters, each spectral channel has between 29 and 37 spectral filters alone. The second consideration is that each combination of spectral bandpass, IWA, and OWA, requires a specific set apodizing, occulting, and Lyot stop masks. Each channel has between 8 and 11 masks combinations to enable different optimized high-contrast regions on the focal plane.

5. HIGH DEFINITION IMAGER (HDI)

5.1 Science Overview and Capabilities

The LUVOIR observatory will revolutionize the study of the formation and evolution of planets, stars, and galaxies. LUVOIR will do this through a combination of very high sensitivity, high angular resolution, and a highly stable and well-calibrated point spread function. A key instrumental capability for LUVOIR is the High Definition Imager (HDI) instrument – the primary astronomical imaging instrument for observations in the near UV through the near IR. Among the key science cases for HDI are:

- Understand the detailed physics of cosmic reionization by measuring the ionizing radiation escape fraction in galaxies as a function of time and environment. This is accomplished via the detection and measurement of Lyman continuum flux for $z \geq 2$ galaxies.
- Study the mechanisms of cosmic reionization by measuring variations, as a function of position on the sky, of the ultra-faint end of the $z \sim 7$ galaxy luminosity function (down to absolute AB magnitude of -12). A drop in the ultra-faint galaxy number density is predicted.
- Reconstruct detailed and accurate star formation histories in many galactic environments not reachable with other facilities by directly detecting stars below the main sequence turn off in all major types of galaxies. This requires reaching out to distances of ~10 Mpc.
- Map the growth of substructure and the evolution galaxy morphology in the era where cosmic star formation peaks ($2 < z < 4$) by observing small-scale structure within $z > 2$ galaxies, down to spatial scales of 100 pc, in the rest-frame UV and visible. In particular, probe the distribution and properties of sub-galactic stellar systems (<100,000 solar masses) over the redshift range $2 < z \leq 10$.

- Constrain the distribution and properties of dark matter by measuring proper motions of stars in Local Group galaxies and by measuring proper motions of galaxies out to nearest groups and clusters within 15 Mpc of Milky Way.
- Search nearby stars for exoplanets via their induced astrometric wobble signature on their host stars to identify systems with Earth-mass planets in HZ regions. This is a potential companion program to the main LUVOIR coronagraphic exoplanet survey.
- Measure the long-term global atmospheric and interior dynamics of the gas and ice giant planets in the outer Solar System. On smaller scales, monitor the changes in surface features and exospheres of small, airless bodies in the Solar System due to volcanic or geyser activity.

These scientific investigations all call for an instrument that can instantaneously observe a field-of-view that spans 6 square arcminutes and provides pixel sampling that takes full advantage of the angular resolution provided by the telescope. The diverse nature of the above science cases (and these are just a few of many), also demand an instrument with an ample range of spectral elements including standard broad, medium, and narrow band filters as well as several dispersing elements to enable low-resolution slitless spectroscopy.

5.2 Design Overview

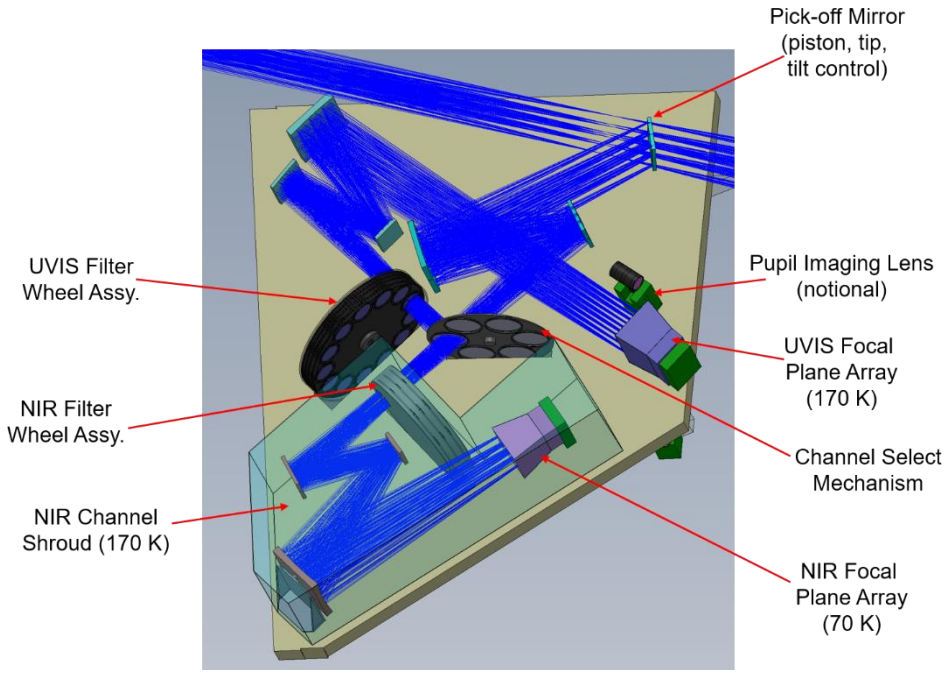

Figure 11 – A rendering of the HDI instrument. Light from the OTE enters from the upper left corner. The rays passing through the pick-off mirror are a rendering artifact and should be ignored. For scale, the UVIS filter wheel assembly is ~1 meter in diameter.

The HDI design provides a 2 x 3 arcminute field-of-view with two channels – an ultraviolet-visible (UVIS) channel covering the range 200 nm – 950 nm and a near-infrared (NIR) channel covering the range 800 nm – 2200 nm. The respective focal plane detector arrays provide Nyquist sampled images at 400 nm (2.73 mas/pixel) for UVIS imaging and at 1200 nm (8.20 mas/pixel) for NIR imaging. The choice to achieve Nyquist sampling is motivated by a desire to maximize information extraction from the images and to enable the best possible image quality when HDI is operating in parallel with other instruments (some of which cannot tolerate dithering maneuvers by the observatory pointing system). In addition, the optical design of the HDI instrument gives the UVIS and NIR channels nearly identical fields-of-view and allows for the option to perform simultaneous observations in both channels. A model of the HDI instrument layout is shown in Figure 11.

The UVIS channel contains a filter select mechanism consisting of 4 wheels, with each wheel capable of holding 13 elements. The design allows for 41 science spectral elements, 4 clear slots (needed to allow access to each set of filters on each wheel), 1 dark slot, 4 defocus lenses, and 2 Dispersed Hartman Sensors (DHS). The NIR channel filter select mechanism consists of 3 wheels with 10 elements per wheel. The current design allows for 26 science spectral elements, 3 clear slots, and 1 dark slot. For both the UVIS and NIR channel, the filters will be selected based on current user preferences, experience with the imagers currently on board HST, and imagers that will be on JWST.

The Channel Select Mechanism (CSM) is a single wheel with 6 positions. The CSM controls the path of the light from the relay optics to the HDI detectors. It also enables light from the internal calibration lamp system to be directed into either of the two channels. The six positions are:

- Clear – send all light from the telescope to the NIR channel. This position also allows light from the internal calibration system to be sent into the UVIS channel.
- Full Reflective – send all light from the telescope into the UVIS channel. The backside of this mirror is also fully reflective, allowing light from the internal calibration system to be sent into the NIR channel.
- 50/50 Beam Splitter – broadband beam splitter for simultaneous UVIS and NIR imaging, albeit with each channel receiving half the light.
- Dichroic Beam Splitter – sends light from the telescope to both the UVIS and NIR channels simultaneously but over a restricted range of wavelengths in each channel, allowing nearly 100% transmission in each of these windows.
- Optimized UV mirror – send all light from the telescope in a defined UV passband into the UVIS channel. Can supersede the need to use a transmissive UV filters for some wavelength ranges of interest in the 200 – 390 nm range.
- Second optimized UV mirror for UVIS only imaging.

Special Modes:

In addition to simultaneous UVIS and NIR imaging, HDI provides three special modes of operation. HDI's precision astrometry mode enables a range of exciting science not feasible on existing telescopes including astrometric detection of exoplanets and measuring proper motions of extragalactic sources in the Local Group and beyond. To achieve the astrometric accuracy required for these applications (±1 micro-arcsecond), we need to calibrate the position of every pixel in the UVIS detector array. Such a metrology calibration system is needed if one wishes to measure galaxy proper motions out at the 10 – 15 Mpc distance scale or to detect the stellar wobble induced by Earth-mass exoplanets orbiting their host main sequence stars. An all-fiber metrology system[31] is included in HDI to allow for the calibration of the UVIS focal plane pixel geometry to a precision of 10^{-4}.

A second special mode of HDI is to function as LUVOIR's primary fine-guidance sensor. Both the UVIS and NIR focal plane have the capability of defining small regions-of-interest (ROIs) around bright foreground stars. These ROIs can be read-out at high speeds (~200 Hz or faster) to provide a pointing signal to the fine-steering mirror and VIPPS. This can be done without interrupting regular science operations.

Finally, the HDI focal plane will serve a function similar to that of NIRCam on JWST, and provide defocused image data for phase retrieval and wavefront sensing[32]. This data will be used during commissioning of the observatory to align and phase the primary mirror segments, as well as during routine maintenance of the wavefront as needed. Six elements in the UVIS filter wheel are dedicated to supporting this mode of operation: 4 weak lenses for generating defocused point-spread function (PSF) data, and 2 dispersed Hartmann sensors (DHS) for performing coarse phasing of the primary mirror segments.

Detectors:

The UVIS channel includes a 2.7 Gigapixel imaging array comprised of forty (40) 8K x 8K detectors arranged in a 5 x 8 pattern. The UVIS detectors are currently envisioned to be CMOS-based devices with 5 micron pixels. The 8K x 8K format for each sensor included in the current design has not yet been produced in flight-qualified scientific systems but is within a realistic technology trajectory from current devices. The assumed read noise is 2.5 e-/pixel and the assumed dark current is 0.002 e-/sec/pixel. A final detector decision, of course, would not need to be made for several years allowing ample time for detector development.

The NIR detectors are envisioned to be a 4 x 5 array of HgCdTe-based devises with 10 micron pixels. The 4K x 4K format for each sensor included in the current design is TRL5, due to the development work on H4RG detectors for the WFIRST mission[33]. We anticipate 4K HgCdTe detectors to be TRL9 with the launch of WFIRST. A 2x improvement in dark current, however, would be desired to achieve LUVOIR sensitivity in the NIR. We are assuming 2.5 e- per pixel readout noise and dark current levels of ~0.002 e-/sec/pixel.

6. LUMOS

6.1 Science Overview and Capabilities

A ubiquitous theme that has emerged in the science definition phase has been the study of gas in the cosmos, its relationship to (and evolution with) star and galaxy formation, and how this gas is transferred from one site to another. Understanding the flow of matter and energy from the intergalactic medium (IGM) to the circumgalactic media (CGM), and ultimately into galaxies where it can serve as a reservoir for future generations of star and planet formation, is essentially a challenge in characterizing the ionic, atomic, and molecular gas at each phase in this cycle. LUVOIR will be capable of characterizing the composition and temperature of this material in unprecedented scope and detail; on scales as large as the cosmic web and as small as the atmospheres of planets around other stars. The common denominator for this science case is that the strongest emission and absorption lines in the gasses to be studied – therefore the highest information content for understanding the physical conditions in these objects – reside at ultraviolet wavelengths, roughly 100 – 400 nm. The LUVOIR Ultra-violet Multi-object Spectrograph (LUMOS) instrument is designed to make revolutionary observational contributions to all of the disciplines that call for high-resolution spectroscopy, multi-object spectroscopy, and imaging in the ultraviolet bandpass. For a more detailed discussion of the LUMOS science case and instrument design, the reader is referred to France, *et al*[34]

6.2 Design Overview

LUMOS is a highly multiplexed ultraviolet spectrograph, with medium and low-resolution multi-object imaging spectroscopy and FUV imaging modes. LUMOS can be thought of as an analog to the successful HST-Space Telescope Imaging Spectrograph (STIS) instrument, with two orders-of-magnitude higher efficiency, multi-object capability, and a wide-field multi-band imaging channel[35]. Coupling the high instrumental throughput with a factor of ~40× gain in collecting area over HST ($[15m / 2.4m]^2 = 40$), LUMOS can reach to limiting fluxes of order 100 – 1000 times fainter than currently possible with the HST Cosmic Origins Spectrograph (COS) and STIS instruments. Figure 12 shows predicted effective area curves for the multi-object spectrograph modes.

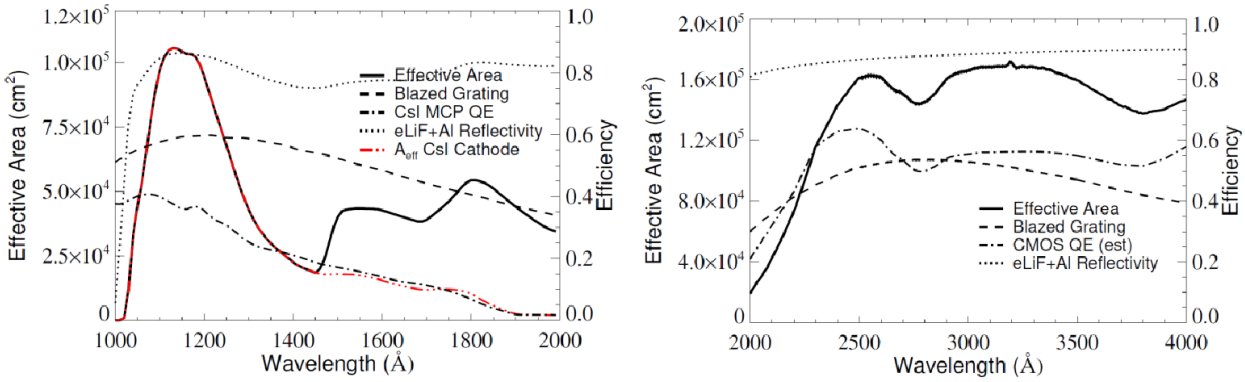

Figure 12 – Effective are of the LUMOS FUV (left) and NUV (right) multi-object spectrograph modes.

Multi-object Imaging Spectroscopy:

Figure 13 shows the layout of the LUMOS multi-object imaging spectroscopy channel. The entrance aperture for the spectrograph is a 3 x 2 grid of microshutter arrays[36] (MSAs). The MSA arrays build on the heritage of the Near Infrared Spectrograph (NIRSPEC) on JWST[37], with 6 individual arrays of 420 x 840 shutters where each shutter has a 100μm x 200μm pitch. The MSA grid defines the field-of-view for multi-object spectroscopy, 3′ × 1.6′ for the FUV modes and 1.3′ × 1.6′ for the NUV mode. In both modes, light passing through the MSA is directed onto a series of six fixed gratings via a fixed convex biconic optic and a second aberration-correcting toroidal steering mirror. Piston, tip, and tilt control of second mirror, selects which of the six gratings is illuminated at any given time.

Of the six fixed gratings, five are used for Far-UV (FUV, 100-200 nm) spectroscopy, and include medium, low, and very low spectral resolution options. The sixth grating provides a medium-resolution Near-UV (NUV, 200-400 nm) option. Table 2 summarizes the spectral resolution, bandpass, angular resolution and field-of-view for each mode of the multi-object spectrograph. All of the FUV MOS modes are focused onto a 2 x 2 array of large-format microchannel plate (MCP) detectors. The NUV MOS mode is focused onto a 3 x 7 array of δ-doped CMOS devices, similar to those used in the HDI UVIS channel.

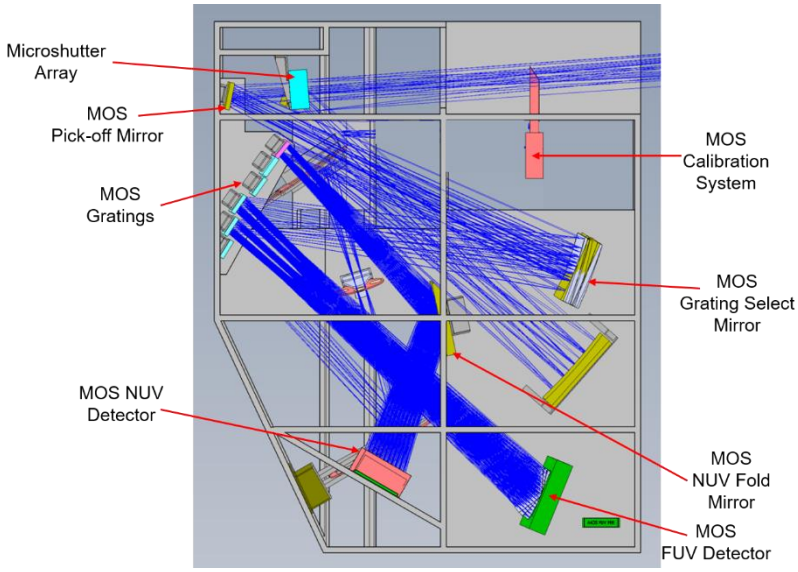

Figure 13 – A rendering of the LUMOS instrument, showing ray paths for both the multi-object spectrograph channel, as well as the imaging channel. Only elements for the multi-object spectrograph channel are annotated, as imaging channel elements are largely hidden behind the bulkheads. Light from the OTE enters from the upper right.

Far-UV Imaging:

The majority of the LUVOIR imaging science is addressed through the HDI instrument (200 nm – 2.5 μm), and LUMOS will provide a complimentary FUV imaging capability from 100 – 200 nm. The LUMOS FUV imaging aperture is physically offset from the MOS MSA aperture (see Figure 5), and light from the OTE enters this channel through an unobstructed open aperture. Figure 14 shows a schematic raytrace of the imaging channel. Two aberration-correcting optics direct the light through two identical reflective filter wheel assemblies that serve to define the imaging bandpass in this mode. A neutral-density filter wheel is also inserted between the two filter wheels to accommodate FUV bright object protection, target acquisition for the MOS channel, and safe imaging of the target field through the MSA for shutter selection. The images are recorded on a single 200 mm x 200 mm MCP detector. Table 2 summarzies the bandpass and angular resolution achieved by the FUV imaging channel.

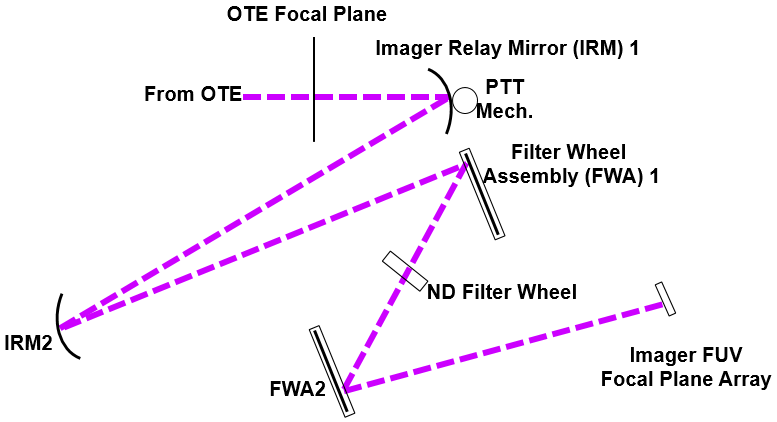

Figure 14 – Schematic block diagram of the LUMOS FUV imaging channel.

Cross-over Mode:

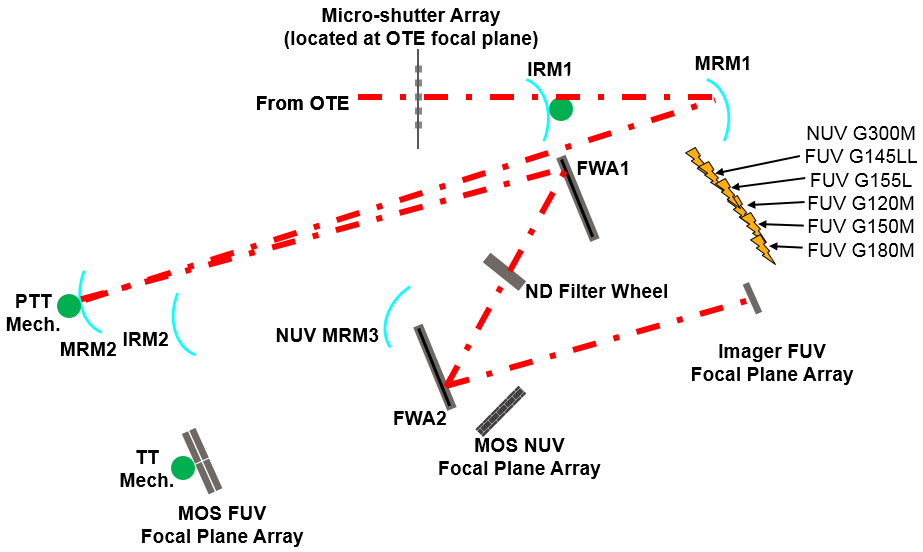

Figure 15 – Schematic block diagram of the "cross-over" mode. Elements from both the imaging channel and multi-object spectrograph channel are shown, and the red dashed-dot line show the beam path entering the MOS channel and crossing over the imaging channel after MRM2.

LUMOS performs bright object protection by pre-imaging the target field through the MSA. LUMOS contains a 'cross-over mode' that uses MRM2 to direct light to FWA1 in the imaging channel, through an ND filter wheel, and to the FUV imaging detector. Figure 15 shows a schematic of the cross-over mode, with elements of both the MOS and imaging channels shown. In this way, target brightness is quantified prior to spectral imaging acquisition with the MOS (imaging target acquisitions can also be made through the ND filter for bright-object-protection in the FUV imaging mode). Imaging the spectroscopic target field through the MSA has a second benefit: it enables autonomous microshutter selection and fine-guidance adjustments to acquire the target through the selected shutter/slit. Operationally, the target field is imaged through the MSA, the user-supplied celestial coordinates are references to local detector x-y coordinates, and the instrument autonomously selects the appropriate sources and determines the fine pointing adjustments that are required to align the primary science target(s) with the appropriate MSAs and these signals are relayed to the flight computer to complete the target acquisition.

Table 2 – The instrument parameter goals specified for each mode by the LUMOS instrument team. In each box where relevant, the target value is shown on top, the average value at the center of the field is shown second in parentheses, and the average value over 80% of the field-of-view is shown third in parentheses and italics. This last value demonstrates that LUMOS achieves the spectral and spatial resolution goals across the majority of its spectral and spatial detector area.

Instrument Parameter	**G120M**	**G150M**	**G180M**	**G155L**	**G145LL**	**G300M**	**FUV Imaging**
Spectral Resolving Power	30,000 (42,000) (*30,300*)	30,000 (54,500) (*37,750*)	30,000 (63,200) (*40,750*)	8,000 (16,000) (*11,550*)	500 (500)	30,000 (40,600) (*28,000*)	N/A
Optimized Spectral Bandpass	100-140 nm (92.5-147.4 nm)	130-170 nm (123.4 - 176.6 nm)	160-200 nm (153.4-206.6 nm)	100-200 nm (92.0-208.2 nm)	100-200 nm	200-400 nm	100-200 nm
Angular Resolution	50 mas (11 mas) (*17 mas*)	50 mas (15 mas) (*19.5 mas*)	50 mas (17 mas) (*24 mas*)	50 mas (15 mas) (*27.5 mas*)	100 mas (32 mas)	50 mas (8 mas) (*26 mas*)	25 mas (12.6 mas) (*12.6 mas*)
Temporal Resolution	1 msec	1 msec	1 msec	1 msec	1 msec	1 sec	1 msec
Field-of-View	2' × 2' (3' × 1.6')	2' × 2' (3' × 1.6')	2' × 2' (3' × 1.6')	2' × 2' (3' × 1.6')	2' × 2' (3' × 1.6')	2' × 2' (1.3' × 1.6')	2' × 2' (2' × 2')

7. ADDITIONAL INSTRUMENTS

In addition to the Coronagraph, LUMOS, and HDI instruments, the LUVOIR STDT has identified compelling science cases for two more instruments. The first, an optical / NIR multi-resolution spectrograph (ONIRS) will be studied in more detail as part of the Architecture "B" design study. Even so, ONIRS would also be a candidate instrument for Architecture "A", just as the three previously discussed instruments are candidates for Architecture "B". The goal is to show flexible instrument and telescope designs that can be combined in multiple configurations to achieve the stated science objectives given programmatic and technical constraints.

The second instrument is being studied by a consortium of European partners, and led by the Centre National d'Études Spatiales (CNES), as part of an international contribution to the LUVOIR Study. This instrument, called Pollux, is complementary to the LUMOS instrument and provides high-resolution far-UV spectropolarimetry.

7.1 ONIRS

The Optical-NIR Spectrograph (ONIRS) will enhance LUVOIR's scientific portfolio by enabling optical and near-infrared spectroscopy at a range of resolutions. The instrument is still under design, but our optimistic plans include broad wavelength coverage, variable spectral resolution (R=100 – 300,000), and high spatial resolution. ONIRS will allow observers to probe the chemical evolution of high-redshift galaxies, study the dynamics and composition of the circumgalactic medium, monitor the expansion of the universe, and measure dynamical masses of black holes. Closer to home, ONIRS will also improve our understanding of star formation and the initial mass function; protostellar outflows and jets; protoplanetary and debris disks; the composition of planets and their atmospheres; asteroids and comets; and planetary surface processes.

Table ***3*** summarizes some of the performance capabilities and driving science cases for ONIRS.

Table 3 – *ONIRS Instrument performance capabilities and driving science requirements.*

Spectral Resolution	**Sample Science Drivers**
Low	Exoplanet transmission spectroscopy (R=200) Pluto surface characterization (R=500)
Medium	White dwarf mass/radius relation (R=10,000) Protoplanetary and debris disks (R=20,000-30,000) Host star characterization (R=30,000)
High	Expansion of the universe (R=100,000) Template matching (R=100,000) Radial velocity mass measurements (R=300,000)
Field of View	**Sample Science Drivers**
Low	Gas in debris disks (20") Protostellar outflows / jets (30")
Medium	Disk wind and mass accretion (2') Star formation and IMF (1' – 2')
High	Comets (2' – 5') High-redshift galaxies (10')
Spatial Resolution	**Sample Science Drivers**
Low / Medium	High-redshift galaxies (0.1") Protoplanetary disks (0.7" – 7")
High	Solar system atmospheres (0.008") Disk wind and mass accretion; protostellar outflows/jets (0.01")

In order to take full advantage of LUVOIR's location in space, ONIRS will need to have exquisite wavelength calibration and stability. The science cases of measuring the masses of planets and the expansion of the universe place the tightest constraints on instrumental performance: the ability to measure signals with amplitudes of a few cm/s over year-long baselines. A laser frequency comb is a likely candidate for a high-precision wavelength calibration source, however additional study is needed to determine the technical feasibility of this solution for a flight instrument.

Due to the desire to acquire time-sensitive observations (e.g., exoplanet spectroscopy during transit or secondary eclipse), the ideal ONIRS design would enable observation across the entire ONIRS bandpass simultaneously. These time-sensitive cases tend to require lower spectral resolution, so a compromise could be to have a choice between broad wavelength coverage with lower spectral resolution (R = 200 – 500) or narrower wavelength coverage at higher spectral resolution (R = 20,000 – 300,000). A second generation upgrade to ONIRS could incorporate broad wavelength coverage at high spectral resolution.

Using ONIRS to probe atmospheres of exoplanets via template matching or measure the masses of black holes will require coupling ONIRS to the coronagraph. The Architecture "A" coronagraph instrument provides a useful case study for such an instrument.

The ONIRS instrument will receive additional study and definition during the next year as part of Architecture "B".

7.2 Pollux

Early in the LUVOIR study process, CNES expressed interest in contributing a full instrument concept study to the Architecture "A" design. CNES assembled a consortium of 10 different labs in 6 different European countries and presented an outline for a high resolution UV spectropolarimeter that will complement the capabilities of LUMOS. The LUVOIR study team provided an interface document with mass, volume, and power allocations for their instrument. The CNES team is currently executing their instrument study and will deliver their final report in late 2018, in time for the LUVOIR final report to be submitted to the 2020 Astrophysics Decadal Survey.

At this early stage, only preliminary information is available about the instrument's capabilities. The instrument covers three bandpasses: the far-UV (FUV, ~90 – 125 nm), the mid-UV (MUV, 115 – 220 nm), and the near-UV (NUV, 210 – 390 nm). The three bands are divided into three separate channels within the instrument. A mechanical flip-in mirror just after the instrument entrance aperture first selects whether light is directed towards the FUV channel, or the MUV/NUV channel. If the MUV/NUV channel is selected, then the field-of-view of the instrument is divided in half, with half being directed to the MUV optics, and half directed to the NUV optics. All channels consist of a polarimeter element, a collimator, an echelle grating, a cross disperser, and a detector tailored to the specific spectral band of interest. Table 4 summarizes the performance requirements and goals of the instrument.

Table 4 – Pollux instrument specifications.

Parameter	**Requirement**	**Goal**
Minimum Wavelength	98 nm	90 nm
Maximum Wavelength	390 nm	400 nm
Spectral Resolution	120,000	200,000
Aperture Size	30 mas	10 mas
Limiting Magnitude	V = 26	
Polarization	Circular + Linear	
Polarization Sensitivity	$10^{-6} – 10^{-11}$	
Radial Velocity Stability	$1/10^{th}$ of a pixel	
Flux Stability	0.001% over 30 hours	
Time Resolution	FUV: 1 s MUV/NUV: 30 s	

8. SPACECRAFT

8.1 Capabilities

The spacecraft must provide basic services to the optical payload: power, communications, attitude control, command and data handling (C&DH), propulsion, and structural support during launch. The spacecraft also thermally isolates the payload from solar heat loads via the sunshield, as discussed in Section 2.1. Each of these subsystems are designed to not only meet the minimum 5-year mission needs, but also anticipate future evolution of the LUVOIR observatory.

8.2 Design Overview

Spacecraft Structure

The spacecraft bus itself is octagonal in shape, and is divided into eight serviceable orbital replacement unit (ORU) bays. A central ninth, non-removable bay holds the propellant tanks, which are refuelable. The central bay is also surround by the primary load-bearing structure, which supports the mass of the payload and transfers that load directly to the launch vehicle during launch and ascent. Each ORU houses one of the main spacecraft subsystems, discussed in more detail below. Additionally, each ORU holds one of the 8 solar panels, allowing the solar array to be upgraded as ORUs are replaced.

Attitude Control System (ACS)

The spacecraft is three-axis stabilized and inertially fixed, with the spacecraft axial vector aligned along the sun-earth axis. The ACS is responsible for counteracting external disturbances (primarily solar pressure torques), as well as changing the yaw axis of the observatory and reacting against gimbal pitch changes during telescope retargeting maneuvers.

An ACS sensor suite consists of star trackers, coarse sun sensors, and proximity sensors on the VIPPS, and determine the attitude of the spacecraft relative to both the payload and the sun. ACS actuators, consisting of eight control moment gyroscopes (CMGs) and twenty 5-lb. thrusters respond to the sensor suite to maintain the attitude. The CMGs are arranged in four sets of two dihedral configurations (a primary and a spare), for full three-axis stabilization. The thrusters are arranged in three sets: the first is used during momentum dump maneuvers, the second is used for station-keeping and orbit maintenance, and the last set is made of long-duration thrusters and is used solely for the orbit insertion burn to enter the SEL2 halo orbit.

Command & Data Handling (C&DH)

The C&DH system consists of a solid state recorder for buffering data during downlinks, a board-level computer for command and control, dedicated controller boards for spacecraft deployment and gimbal mechanisms, and a separate ACS safehold processor which takes over in the event of a C&DH system failure. All components are redundant and cross-strapped.

Communications

The primary communications system uses a standard Ka-band high gain antenna, using a near-Earth network (NEN) downlink to ground stations in White Sands, NM, and South Africa. While the Ka-band system provides adequate margin for LUVOIR's anticipated data volumes, an optical communication system would provide additional room for growth. Should there be investment in new optical communications ground systems, LUVOIR could easily adopt this high technology readiness solution.

Electrical Power Systems

To provide more than 10 kW of power needed by the LUVOIR payload, ~80 m^2 of solar panels is needed. The solar array is divided into eight panels, one for each of the eight ORUs. When deployed, the solar panels make a "mini" sunshield which helps shadow the stowed payload immediately after initial ascent until after the first mid-course correction when the full sunshield can be deployed; a battery is included solely for providing power during launch and ascent. The power system provides 28-v to spacecraft subsystems, and 120-v directly to the payload.

Propulsion

In addition to the array of 5-lb. thrusters described in the ACS section, a single 100-lb. thruster is included for the first mid-course correction maneuver. This maneuver occurs ~12 hours after launch and primarily corrects the trajectory for variability in the launch vehicle performance.

Flight Dynamics

LUVOIR will orbit the second Sun-Earth Lagrange (SEL2) point in a quasi-halo orbit that does not exceed 25° from the Sun-Earth axis at its maximum, or 5° from the Sun-Earth axis at its minimum.

Reliability

Throughout the LUVOIR observatory (both the spacecraft and the payload) a minimum risk acceptance posture was adopted. All electrical system boards are side-A / side-B redundant, all mechanisms have dual-windings, and all electrical power and data interfaces are either cross-strapped, redundant, or both.

9. FUTURE WORK

While the LUVOIR Architecture "A" concept has completed its primary design effort, a number of tasks still need to be completed to finalize the concept:

- The sunshield requires additional design to finalize specific details regarding the number of layers, layer separation, layer angle, and material properties;
- A dynamic integrated model is being developed to analyze the dynamic wavefront stability that can be achieved by the VIPPS active isolation architecture;
- A complete observatory-level thermal model is being finalized to support the design of the sunshield, verify radiator allocations on the instrument modules, and inform technology development efforts for new thermal sensing and control approaches;
- An end-to-end error budget is being developed to allocate wavefront error and wavefront error stability to each subsystem, and inform technology development efforts in support of achieving picometer-level wavefront stability;
- Control systems modeling is underway to coordinate interactions between the primary mirror edge sensors, segment actuators, coronagraph low-order and out-of-band wavefront sensors, coronagraph deformable mirrors, and VIPPS; and
- Compile a complete master equipment list for the entire observatory to support independent cost assessments that will be performed both by the study office and by the 2020 Decadal Survey.

As the LUVOIR Study Team continues to work on these tasks, the team will also soon begin studying the second architecture, a 9-m class telescope, with similar instrument capabilities (although likely different instrument designs), designed to fit within mass and volume constraints consistent with today's state-of-the-art fleet of heavy launch vehicles.

REFERENCES

[1] P. Hertz, "Charter for the Mission Concept Study Science and Technology Definition Teams," NASA, 28 December 2015, https://science.nasa.gov/astrophysics/2020-decadal-survey-planning/ (accessed 29 August 2017).

[2] "The Habitable Exoplanet Imaging Mission (HabEx)," Jet Propulsion Laboratory, https://jpl.nasa.gov/habex/ (accessed 29 August 2017).

[3] R. G. Lyon and M. Clampin, "Space telescope sensitivity and controls for exoplanet imaging," *Opt. Eng.* **51**(1), 011022 (2012).

[4] S. B. Shaklan, *et al.*, "Stability error budget for an aggressive coronagraph on a 3.8 m telescope," *Proc. SPIE* **8151**, 815109 (2011).

[5] M. T. Stahl, *et al.*, "Effects of space telescope primary mirror segment errors on coronagraph instrument performance," *Proc. SPIE* **10398**, 1039816 (2017).
[6] M. J. Eisenhower, *et al.*, "ATLAST ULE mirror segment performance analytical predictions based on thermally induced distortions," *Proc. SPIE* **9602**, 96020A (2015).
[7] S. C. Park, *et al.*, "LUVOIR backplane thermal architecture development through the composite CTE sensitivity study," *Proc. SPIE* **10398**, 1039814 (2017).
[8] L. D. Dewell, *et al.*, "Dynamic stability with the disturbance-free payload architecture as applied to the Large UV/Optical/Infrared (LUVOIR) mission," *Proc. SPIE* **10398**, 1039812 (2017).
[9] F. Shi, *et al.*, "Testbed demonstration of low-order wavefront sensing and control for WFIRST coronagraph," *Proc. SPIE* **10400**, 1040013 (2017).
[10] L. D. Feinberg, *et al.*, "Ultra-stable segmented telescope sensing and control architecture," *Proc. SPIE* **10398**, 1039827 (2017).
[11] J. B. Jewell, *et al.*, "Optimization of coronagraph design for segmented aperture telescopes," *Proc. SPIE* **10400**, 1040017 (2017).
[12] N. T. Zimmerman, *et al.*, "Apodized/shaped pupil Lyot coronagraph designs for segmented aperture space telescopes," *Proc. SPIE* **10400**, 1040018 (2017).
[13] Q. Gong, *et al.*, "Further exoplanet suppression using microlens/pinhole mask for LUVOIR coronagraph," *Proc. SPIE* **10400**, 1040061 (2017).
[14] L. D. Feinberg, "LUVOIR Telescope Temperature Considerations", *LUVOIR Tech Notes*, 5 August 2016, https://asd.gsfc.nasa.gov/luvoir/tech/LUVOIR_Tech_Notes/ColdTemperatureTelescopeConsiderations.pdf (accessed 29 August 2017).
[15] "Space Launch System (SLS) Mission Planner's Guide, ESD 30000, Release Date 04/12/17", NASA NTRS, 12 April 2017, https://ntrs.nasa.gov/search.jsp?R=20170005323 (accessed 29 August 2017).
[16] C. C. Stark, *et al.*, "Lower Limits on Aperture Size for an ExoEarth Detecting Coronagraphic Mission," *The Astrophysical Journal* **808**, 149 (2015).
[17] See https://asd.gsfc.nasa.gov/luvoir/tools/
[18] L. Pueyo, "The LUVOIR Coronagraph Instrument: Definition and Design," *Proc. SPIE* **10398**, 1039815 (2017).
[19] F. Shi, *et al.*, "Low order wavefront sensing and control for WFIRST coronagraph," *Proc. SPIE* **9904**, 990418 (2016).
[20] B. Nemati, *et al.*, "The effect of radiation-induced traps on WFIRST coronagraph detectors," *Proc. SPIE* **9915**, 99150M (2016).
[21] B. Nemati, "Detector selection for the WFIRST-AFTA coronagraph integral field spectrograph," *Proc. SPIE* **9143**, 91430Q (2014).
[22] B. A. Macintosh, *et al.*, "The Gemini Planet Imager: from science to design to construction," *Proc. SPIE* **7015**, 710518 (2008).
[23] J.-L. Beuzit, *et al.*, "SPHERE: a planet imager for the VLT," *Proc. of the Conf. In the Spirit of Lyot 2010*, 44 (2010).
[24] S. Hinkley, *et al.*, "A new high contrast imaging program at Palomar observatory," *Pub. of the Astr. Soc. of the Pacific* **123**(899), 74-86 (2011).
[25] R. T. Demers, *et al.*, "Requirements and design reference mission for the WFIRST/AFTA coronagraph instrument," *Proc. SPIE* **9605**, 960502 (2015).
[26] D. Mawet, *et al.*, "Observing Exoplanets with High-dispersion Coroangraphy II: Demonstration of an Active Single-Mode Fiber Injection Unit," *Astrophysical Journal* **838**, 92 (2017).
[27] I. A. G. Snellen, *et al.*, "Fast spin of the young extrasolar planet β Pictoris b," *Nature* **509**, 63-65 (2014).
[28] J. Wang, *et al.*, "Observing Exoplanets with High Dispersion Coronagraphy I: The Scientific Potential of Current and Next-Generation Large Ground and Space Telescopes," *Astronomical Journal* **153**, 183 (2017).
[29] I. A. G. Snellen, *et al.*, "Combining high-dispersion spectroscopy with high contrast imaging: Probing rocky planets around our nearest neighbors," *Astronomy & Astrophysics* **576**, A59 (2015).
[30] K. Cahoy, *et al.*, "CubeSat deformable mirror demonstration," *Proc. SPIE* **8442**, 84424F (2012).
[31] A. Crouzier, *et al.*, "A detector interferometric calibration experiment for high precision astrometry," *Astronomy & Astrophysics*, **595**, A108 (2016).
[32] D. Aronstein, *et al.*, "Phase retrieval algorithm for JWST Flight and Testbed Telescope," *Proc. SPIE* **6265**, 626511 (2006).
[33] D. Content, *et al.*, "Wide field instrument preliminary design for the Wide Field Infrared Survey Telescope," *Proc. SPIE* **8860**, 88600F (2013).

[34] K. C. France, *et al.,* "The LUVOIR Ultraviolet Multi-Object Spectrograph (LUMOS): instrument definition and design," *Proc. SPIE* **10397**, 1039739 (2017).
[35] K. France, "CHISL: the combined high resolution and imaging spectrograph for the LUVOIR surveyors," *JATIS* **2**, 1203, (2016).
[36] M. J. Li, *et al.*, "JWST microshutter array system and beyond," *Proc. SPIE* **7594**, 75940 (2010).
[37] A. S. Kutyrev, *et al.*, "Microshutter arrays: high contrast programmable field masks for JWST NIRSpec," *Proc. SPIE* **7010**, 70103 (2008).